

Ocean and Sea Ice SAF

Technical Note
SAF/OSI/CDOP3/KNMI/TEC/RP/298

Oceansat-2 L2 winds Data Record validation report

25 km and 50 km wind products (OSI-153-a and OSI-153-b)
DOI: 10.15770/EUM_SAF_OSI_0010, 10.15770/EUM_SAF_OSI_0011

Anton Verhoef, Jur Vogelzang and Ad Stoffelen
KNMI

Version 1.1

June 2017

DOCUMENTATION CHANGE RECORD

Issue / Revision	Date	Change	Description
Version 1.0	Apr 2017		Initial version
Version 1.1	Jun 2017	Minor	Changes resulting from comments in DRR

KNMI, De Bilt, the Netherlands

Reference: SAF/OSI/CDOP3/KNMI/TEC/RP/298

Contents

1	Introduction	4
2	Backscatter data stability.....	5
3	Quality Control characteristics.....	6
4	Comparison of winds with NWP model and buoys	7
4.1	<i>NWP model wind comparisons</i>	<i>7</i>
4.2	<i>Buoy wind comparisons</i>	<i>9</i>
5	Triple collocation results.....	13
6	Conclusions.....	15
7	References	16
8	Abbreviations and acronyms.....	18
9	Appendix A: List of used buoys	19

1 Introduction

The EUMETSAT Ocean and Sea Ice Satellite Application Facility (OSI SAF) produces a range of air-sea interface products, namely: stress-equivalent wind, sea ice characteristics, Sea Surface Temperatures (SST) and radiative fluxes, Surface Solar Irradiance (SSI) and Downward Long wave Irradiance (DLI). The Product Requirements Document [1] provides an overview of the committed products and their characteristics in the current OSI SAF project phase, the Service Specification Document [2] provides specifications and detailed information on the services committed towards the users by the OSI SAF in a given stage of the project.

This report contains validation information about the Oceansat-2 OSCAT scatterometer wind Climate Data Record (CDR), produced in the OSI SAF. The archived near-real time ISRO Oceansat-2 level 1b files [3], spanning the period of 15th December 2009 to 20th February 2014 have been kindly provided by NASA's Jet Propulsion Laboratory (JPL) from their archive. The data have been processed using the Pencil beam Wind Processor (PenWP) software version 2.1, as available in the Numerical Weather Prediction (NWP) SAF [4]. More information about the processing and the products can be obtained from the Product User Manual [5].

The quality and stability of the OSCAT wind CDR has been assessed by looking both at backscatter and wind data. Section 2 describes the checks on the backscatter stability over time. Section 3 assesses the Quality Control applied in the products. In section 4, the winds are compared with NWP model data and with wind data from in situ buoys. Section 5 describes triple collocation results to assess the quality of winds from scatterometer, NWP model and buoys separately. Section 6 summarises the main conclusions.

Acknowledgement

ISRO has kindly provided the near-real time OSCAT level 1b data which were used as input for the OSI SAF wind products. JPL have kindly provided their archived OSCAT data record to the OSI SAF.

We are grateful to Jean Bidlot of ECMWF for helping us with the buoy data retrieval and quality control.

2 Backscatter data stability

A very important task when creating climate data records is to check the stability over time of the used instruments. In the scope of this work we have limited ourselves to looking at the radar backscatter (σ^0) on selected locations of the Earth which are known to have stable geophysical properties. Kumar et al. [6] have looked at SeaWinds backscatter responses over deserts, rain forests and snow covered areas. They found that particularly the snow covered areas show a very stable backscatter with very small standard deviations over time (they studied the 2005-2006 period) and little azimuthal variations. We have looked into the backscatter data over the entire period from December 2009 to February 2014 in a snow covered area also used in [6]: a $2^\circ \times 2^\circ$ box centred at 77 S, 126 E (Antarctica). Based on our experience with QuikSCAT data [9], we consider the Antarctica region to be more stable in the long term than the Greenland region used in [6]. Long and Drinkwater describe Antarctic backscatter conditions and their anisotropy in [7]. On Greenland melting events occur during the summer, which will definitely influence the radiometric properties of the snow cover.

In order to monitor the instrument, we have taken the backscatter data on 25 km Wind Vector Cell (WVC) level for all overpasses in each month. HH-polarized and VV-polarized and fore and aft beam data have been considered separately. The data for each month, i.e., all backscatter data acquisitions located within the selected box, have been averaged. In this way, we average out diurnal variations and variations due to different flight directions in multiple orbits over one day. Still we can very well establish the backscatter variations over longer time scales. During the Oceansat-2 mission, an instrument calibration change occurred between 19th and 20th August 2010, which was also reported in literature [8]. For an unknown reason, the σ^0 values dropped by approximately 0.5 dB. This change was corrected in the wind processing, see the section on backscatter calibration in the Product User Manual [5]. It was also accounted for when the backscatter stability over ice was assessed.

Figure 1 shows the backscatter variations over time in the Antarctic area. We see that the σ^0 values show some small seasonal variability. There also appears to be some anisotropy, we observe a difference of approximately 0.1 to 0.3 dB between fore and aft beams of the same polarisation in line with [6]. The long term trends seem to be quite small, apart from the year 2010 where the σ^0 values are ~ 0.2 dB higher for HH and ~ 0.4 dB higher for VV. The reason for this is not clear. The σ^0 drop in August 2010 was corrected for in Figure 1 and with these corrections the wind speed biases appear to be not very different in 2010 as compared to other years, see section 4. A geophysical cause remains possible, but the analogous plots of ASCAT σ^0 values (in the less sensitive C-band) [9] do not show deviations in 2010 and the effect appears exclusively for VV.

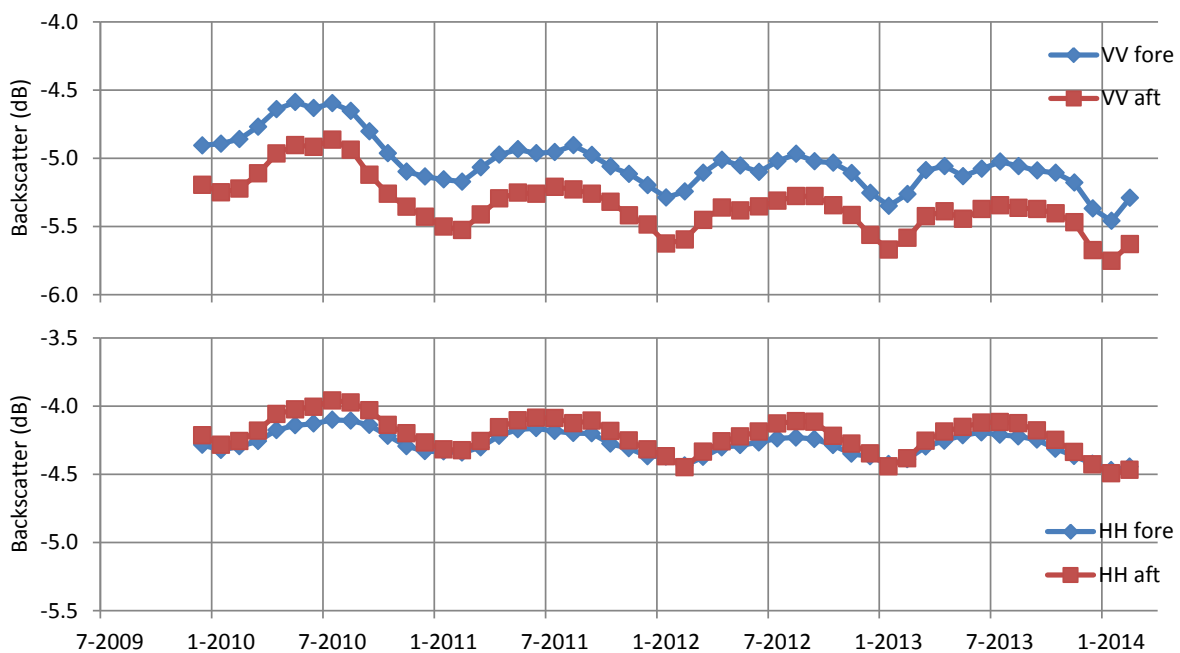


Figure 1: Temporal variation of OSCAT for HH-polarized σ^0 (top) and VV-polarized σ^0 (bottom) over Antarctica (77 S, 126 E).

3 Quality Control characteristics

A good assessment of the information content of scatterometer winds is particularly important in order to use them in weather and climate analysis. Besides retrieval problems in cases of a confused sea state, a particularly acute problem of Ku-band scatterometry is the sensitivity to rain. Elimination of poor quality data is therefore very important for the successful use of the wind data. As part of the OSCAT data record validation, we have investigated the geographical distribution of the rejection fraction of WVCs. We have done this for the year 2010 and for the year 2013. In this way we can see if the rejection rates have logical patterns which can be associated with rainy or dry areas and if there are any changes over time which can be attributed to instrument drifts.

Inspection of Figure 2 reveals that the main areas with high rain rejection rates can be associated with east-west oriented bands in the tropics, most notably in the western Pacific. These are regions known to have strong convection and rain. The bands with high rejection rates near the edges of the Arctic and Antarctic sea ice shelves can be associated with the freezing seasons. When the ice edge rapidly moves due to freezing, the area may be partially covered with sea ice, which is not assigned as ice by the Bayesian ice screening. Particularly in areas with few sea points over the year, sampling noise will appear too in the fraction of Figure 2. Some of these WVCs are rejected by the Quality Control, but they are assigned as 'rain' rather than 'ice'. It is also clear from the plots that the patterns in 2010 and 2013 differ somewhat, particularly near Indonesia and the Atlantic ITCZ.

The collocation of the OSCAT winds with ERA-Interim winds offers the opportunity to compare the climatology of the rejected and accepted points to investigate the effect of QC on climate user metrics and indices. Moreover, the climatology of ERA-Interim sampled by OSCAT may be compared to a homogeneously sampled ERA climatology, to provide an attribution of sampling errors by OSCAT in the user metrics and climate indices. For Ku-band scatterometers, such errors are not negligible due to the effect of rain QC.

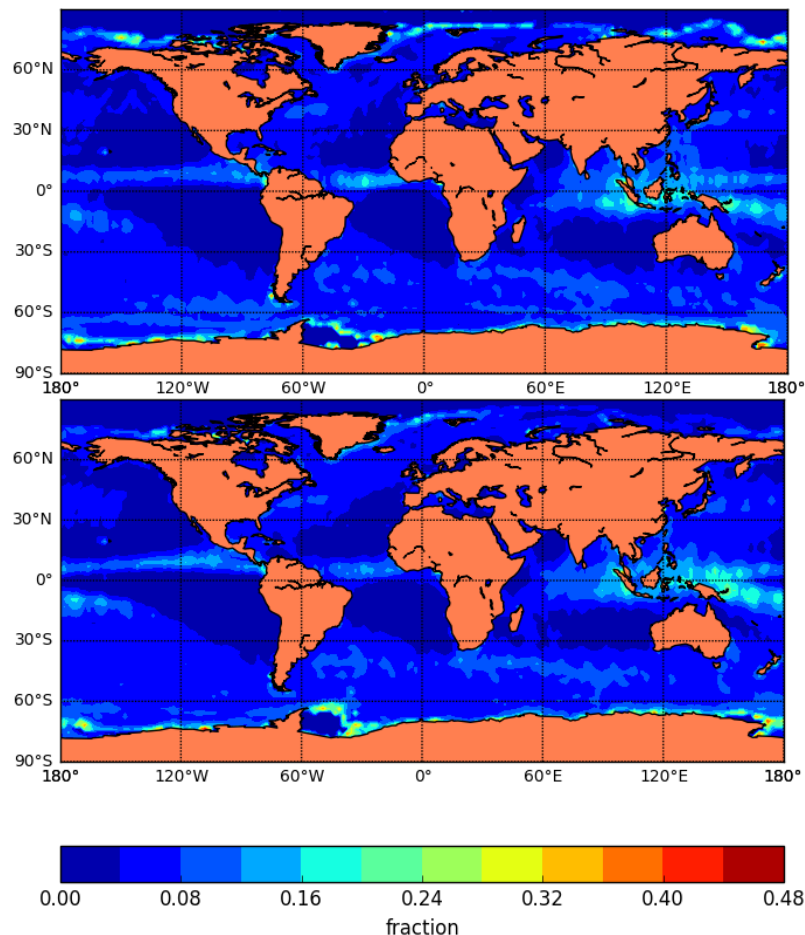


Figure 2: Number of WVCs with KNMI Quality Control (including rain) flag set as a fraction of WVCs where land flag and ice flag are not set. Results are for the entire year 2010 (top) and for the entire year 2013 (bottom).

4 Comparison of winds with NWP model and buoys

4.1 NWP model wind comparisons

The OSCAT scatterometer winds have been collocated with ECMWF re-analysis (ERA) Interim wind data [10]. Stress equivalent (U10S) winds have been computed from the real ERA-Interim forecast 10m winds, sea surface temperature, air temperature, Charnock parameter, specific humidity and mean sea level pressure, using a stand-alone implementation of the ECMWF model surface layer physics [11]. The model wind data have been quadratically interpolated with respect to time and bi-linearly interpolated with respect to location and put into the level 2 information part of each WVC. These model winds have been used both to initialise the Ambiguity Removal step in the wind processing and to monitor the scatterometer winds.

Figure 3 shows the monthly averages of U10S wind speed bias and standard deviations of the zonal and meridional wind vector components over the entire period of the reprocessed data set. The wind speed bias is constant within 0.1 m/s over time; with a gradual decrease over time. The decrease is contrary to what we found for the ASCAT wind speed bias vs. ERA-Interim U10S winds, this showed a flat to slightly increasing trend over the period 2010 to 2013 [9]. Moreover, ASCAT-A winds have been found to be very stable within 0.05 dB or m/s, using a method called cone metrics [12]. The wind vector component standard deviations are fairly constant in time. In the SeaWinds reprocessing we found that the quality of the ERA-Interim U10S winds gradually improves with time in the SeaWinds

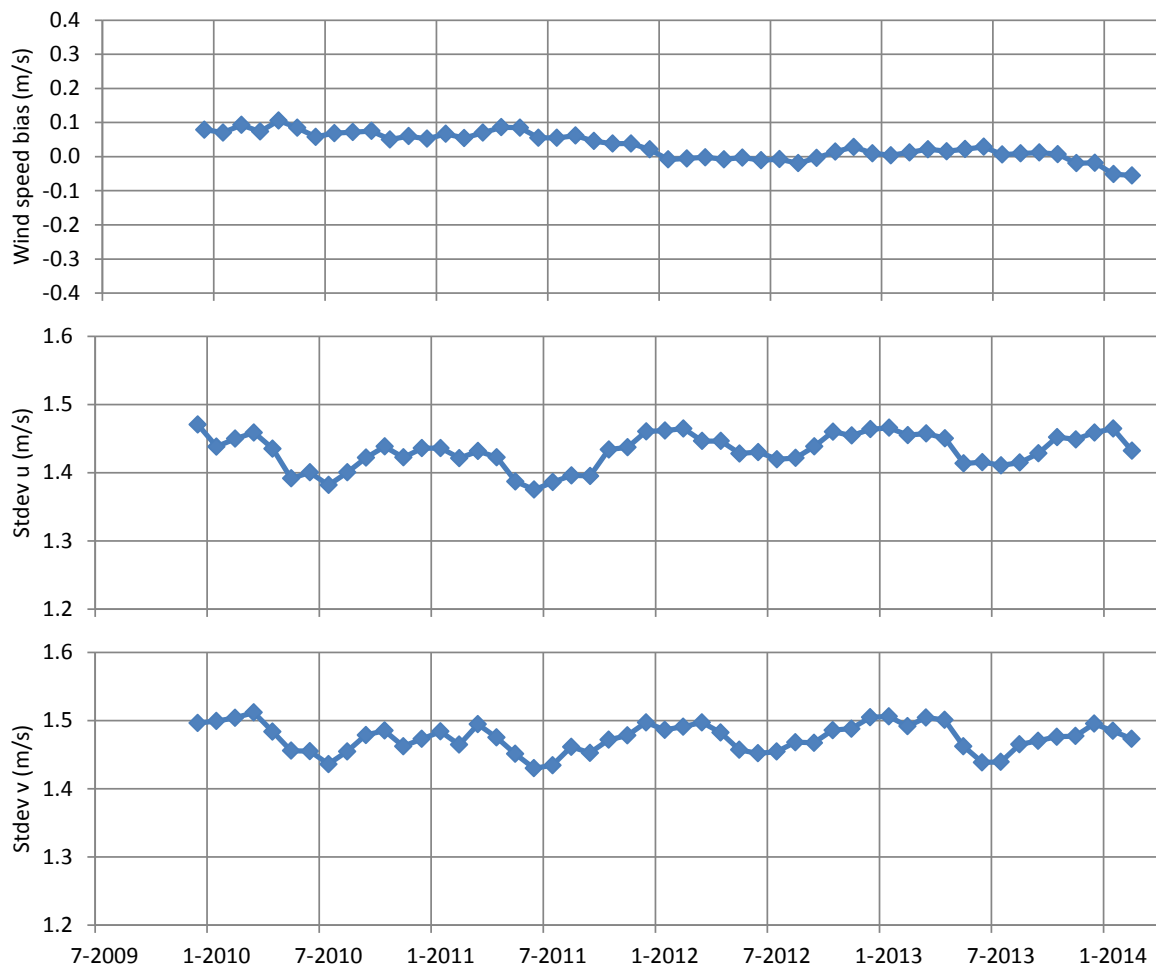


Figure 3: Stress-equivalent wind speed bias (top), standard deviation of zonal wind component (middle) and standard deviation of meridional wind component (bottom) of 25 km OSCAT winds versus ECMWF ERA-Interim model U10S wind forecasts. The plotted values are monthly averages.

era (1999 to 2009) due to the availability of more and more satellite observations which are successfully assimilated into the ERA-Interim model. Assuming constant OSCAT wind quality, ERA-Interim quality appears constant in the OSCAT time frame, however. Note that no scatterometer winds of any instrument were assimilated in ERA-Interim in the period from 2010 onwards. The OSCAT wind component standard deviations are approximately 0.05 to 0.10 m/s higher than those from SeaWinds [9]. We attribute this to higher noise levels of the OSCAT instrument.

In order to better understand the variations in wind speed bias, we have plotted the monthly averages of the scatterometer and model wind speeds separately in Figure 4. It is clear that OSCAT wind speeds decrease by approximately 0.10 to 0.15 m/s from 2010 to beginning of 2014. ERA-Interim wind speeds also decrease, but to a lesser extent. So the wind speed bias decrease in Figure 3 (top) can be explained mainly by the decrease of the OSCAT wind speeds. Note that the model winds are collocated winds and hence the plot does not represent all ERA-Interim winds, but only those at the time and location of Oceansat-2 overpasses. ASCAT winds and accompanying ERA-Interim winds appear to be quite constant in time over this period [9]. The differences in trends between ASCAT and OSCAT are not easy to explain, but we can think of two possible causes. Firstly, the overpass times are different (9:30/21:30 local time for Metop vs. 0:00/12:00 local time for Oceansat-2). Long term climatological trends may be different at different times of the day. Secondly, there may still be small instrument drifts, like the feature in the backscatter over ice in Figure 1, which cause trends in wind climatologies. The operation period of Oceansat-2 is too short and the trends are too small to conclude about this.

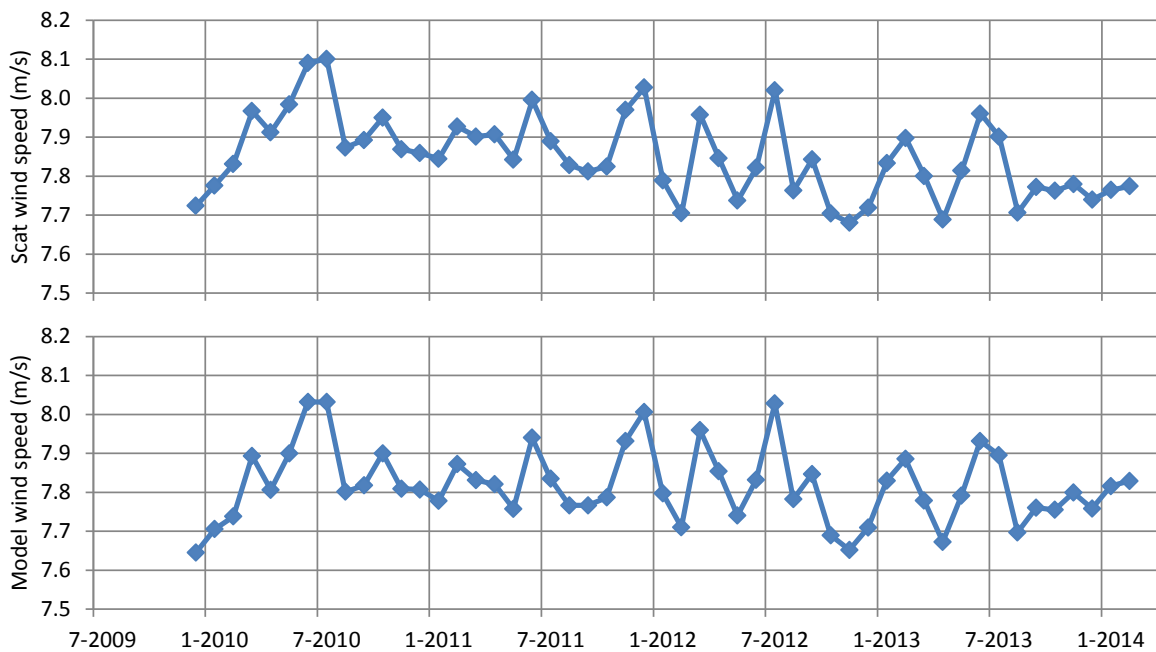


Figure 4: Average OSCAT wind speed (top) and collocated ERA-Interim U10S wind speed (bottom) of 25 km OSCAT winds. The plotted values are monthly averages.

Figure 5 shows the model comparisons for the 50 km OSCAT wind product. The wind speed bias looks almost the same as the 25 km wind speed bias. The 50 km standard deviations are smaller by approximately 0.15 m/s as compared with the 25 km standard deviations but show the same features and trends. The smaller standard deviations are due to the limited spatial resolution of the ERA-Interim winds. The 25 km wind product resolves small scale features which are to a lesser extent present in the 50 km product and absent in the NWP model. Hence it can be expected that the 50 km scatterometer winds closer resemble the model winds and that the standard deviations are smaller.

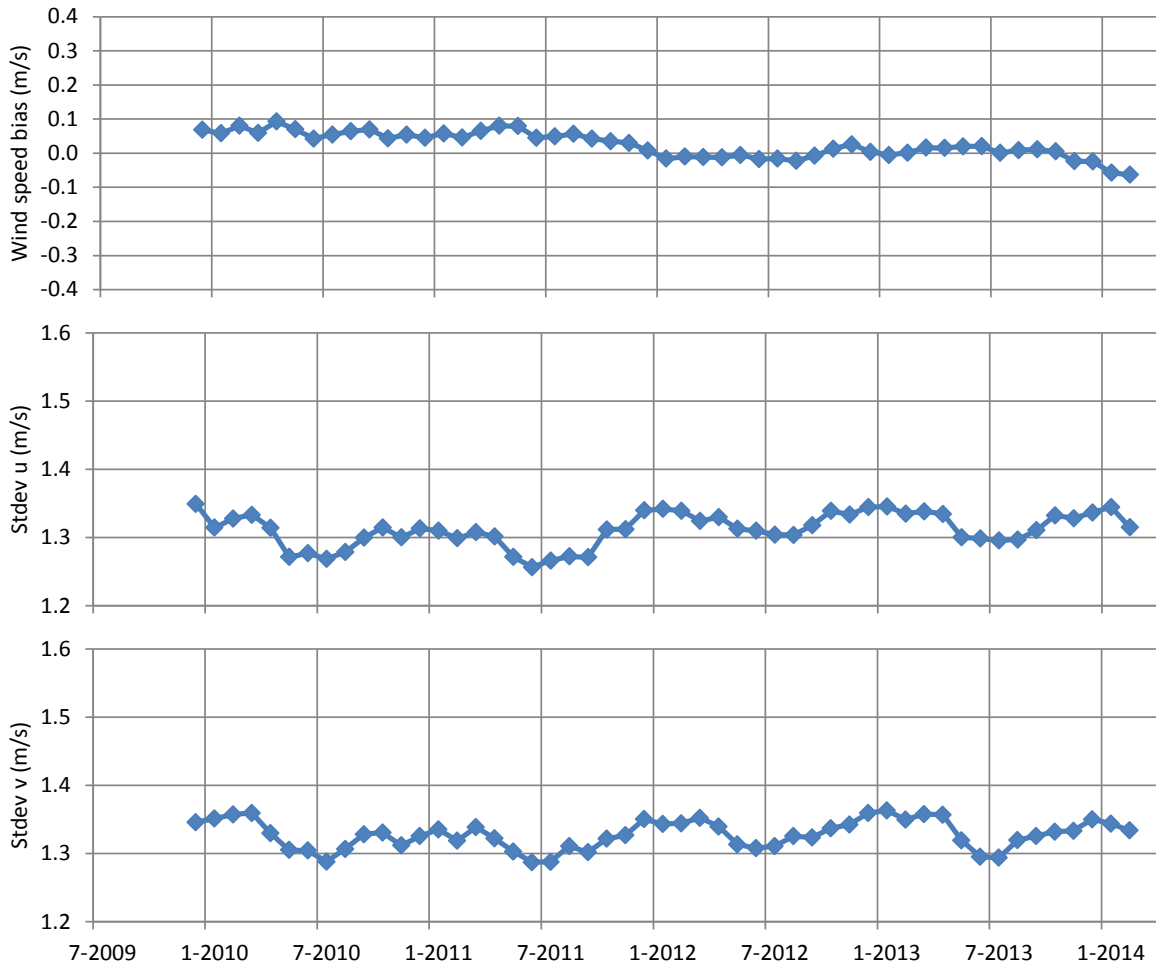


Figure 5: Wind speed bias (top), standard deviation of zonal wind component (middle) and standard deviation of meridional wind component (bottom) of 50 km OSCAT winds versus ECMWF ERA-Interim model wind forecasts. The plotted values are monthly averages.

4.2 Buoy wind comparisons

In this report, scatterometer wind data are compared with in situ buoy wind measurements. The moored buoy winds are distributed through the Global Telecommunication System (GTS) and have been retrieved from the ECMWF MARS archive. The buoy data are quality controlled and (if necessary) blacklisted by ECMWF [13]. The buoy winds are measured hourly by averaging the wind speed and direction over 10 minutes. The real winds at a given anemometer height have been converted to 10-m equivalent neutral winds using the Liu, Katsaros and Businger (LKB) model ([13], [14]) in order to enable a good comparison with the 10-m scatterometer winds. Note that the difference between equivalent neutral winds and stress equivalent scatterometer winds is very small on average [15] so that both may be directly compared.

A scatterometer wind and a buoy wind measurement are considered to be collocated if the distance between the WVC centre and the buoy location is less than the WVC spacing divided by $\sqrt{2}$ and if the acquisition time difference is less than 30 minutes. Note that the collection of available buoy data changes over time: buoys are removed, temporarily or permanently, whereas on the other hand new buoys are deployed on new locations. In order to rule out variations in representativeness, we have taken a sub-set of the available buoys, containing only buoys that have produced wind data in all four years from 2010 to 2013. The approximately 100 buoys used in the validation are listed in Appendix A and a map of the buoy locations can also be found there.

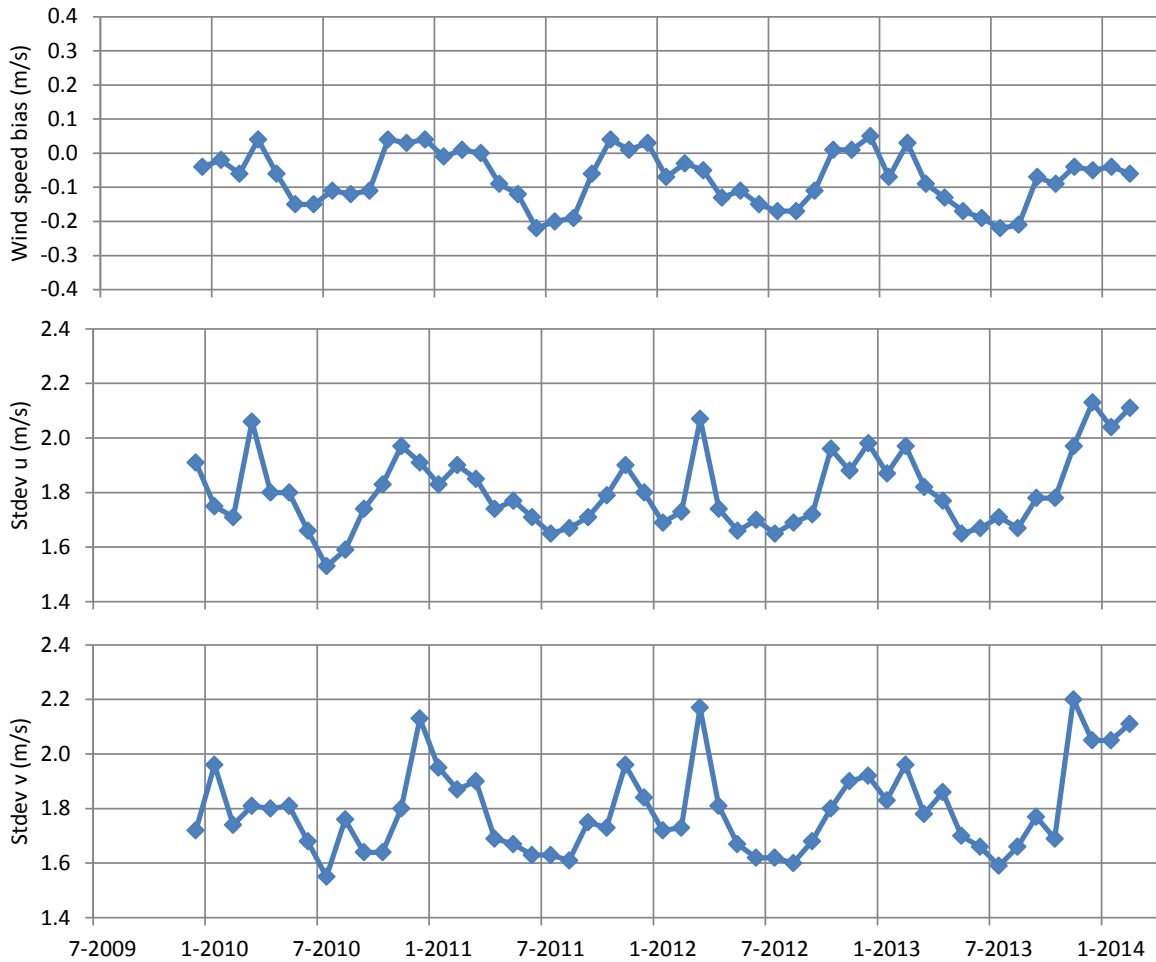


Figure 6: Wind speed bias (top), standard deviation of zonal wind component (middle) and standard deviation of meridional wind component (bottom) of 25 km OSCAT winds versus U10N buoy winds. The plotted values are monthly averages.

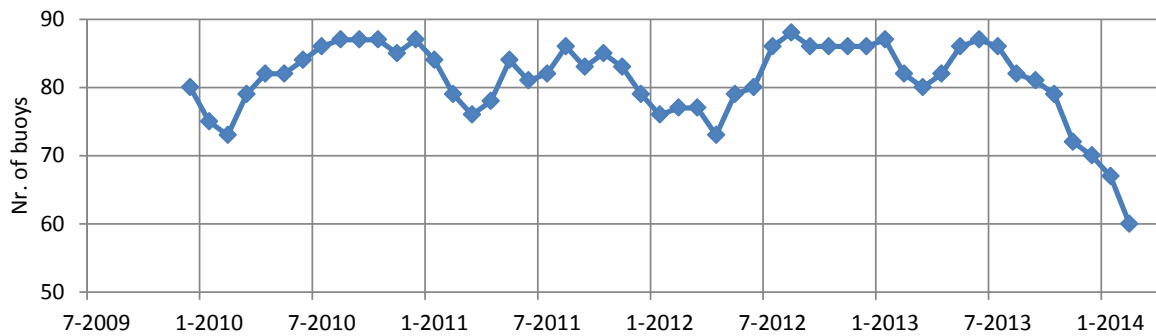


Figure 7: Number of buoys used in the buoy collocations per month.

Figure 6 shows the wind statistics of OSCAT winds versus buoy winds and Figure 7 shows the monthly number of buoys available for collocations, which varies by up to 10% over most of the time, except for the last few months of the mission period, where a more significant decrease is observed. A yearly oscillation is visible for the wind speed bias and wind component standard deviations. Seasonal weather variations cause differences in the probability distribution function of wind speeds. These differences are associated with variations in the spatial representativeness errors of the buoy winds for scatterometer wind validation over a WVC and thereby variations in the difference statistics.

The seasonal oscillations are significantly less prominent in the comparisons with model wind data in the previous section. From our previous work on ASCAT and SeaWinds [9], we know that such oscillations are much stronger in the extratropical areas than in the tropical areas due to larger yearly variations in the weather conditions. This is also the case for the extratropical OSCAT winds (not shown).

The wind component standard deviations in Figure 6 seem to increase over time, especially at the end of the period, but those trends are small as compared to the spread of the points and therefore not significant. The average OSCAT zonal (u) and meridional (v) component standard deviations are 1.8 and 1.8 m/s, respectively. This is slightly higher than the results for ASCAT (1.6 and 1.6 m/s) and SeaWinds (1.7 and 1.7 m/s).

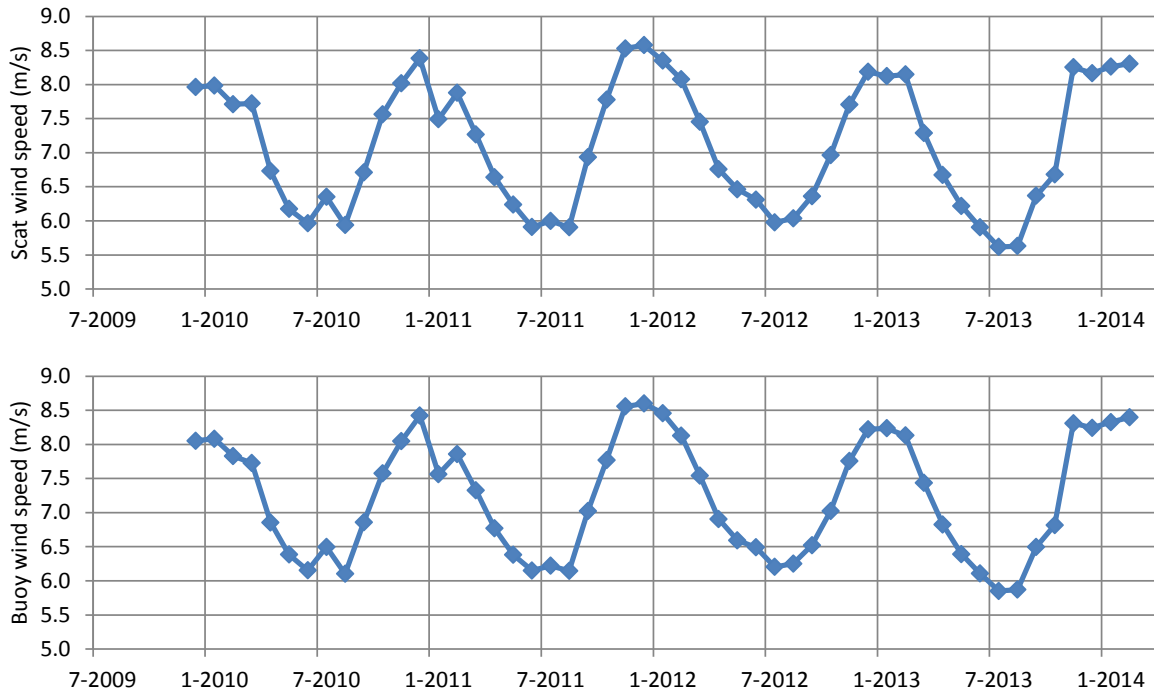


Figure 8: Average 25 km OSCAT wind speed (top) and collocated U10N buoy wind speed (bottom).

The top plot in Figure 6 shows that the wind speed bias of scatterometer winds versus buoy winds slightly decreases over the reprocessing period, just like the wind speed bias versus ERA-Interim winds (Figure 3 top). Analogous to Figure 4, we have plotted the monthly averages of the scatterometer and buoy wind speeds separately, see Figure 8, which show rather large spread and small trends.

Figure 9 shows the buoy comparisons for the 50 km OSCAT products. The results very much resemble the 25 km statistics (Figure 6). The 50 km standard deviations are comparable or slightly lower than the 25 km standard deviations. For SeaWinds and ASCAT we found higher standard deviations for coarser resolution products [9] which is explained by the fact that the buoy winds are point measurements whereas the scatterometer winds are spatial averages over approximately the size of a WVC. Since finer resolution scatterometer products resolve smaller scale features than coarser resolution products, it can be expected that the 25 km OSCAT winds better resemble the buoy winds, resulting in lower standard deviations. Our results show higher standard deviations at 25 km and we attribute this to the noisier wind retrievals from OSCAT as compared to other Ku-band systems.

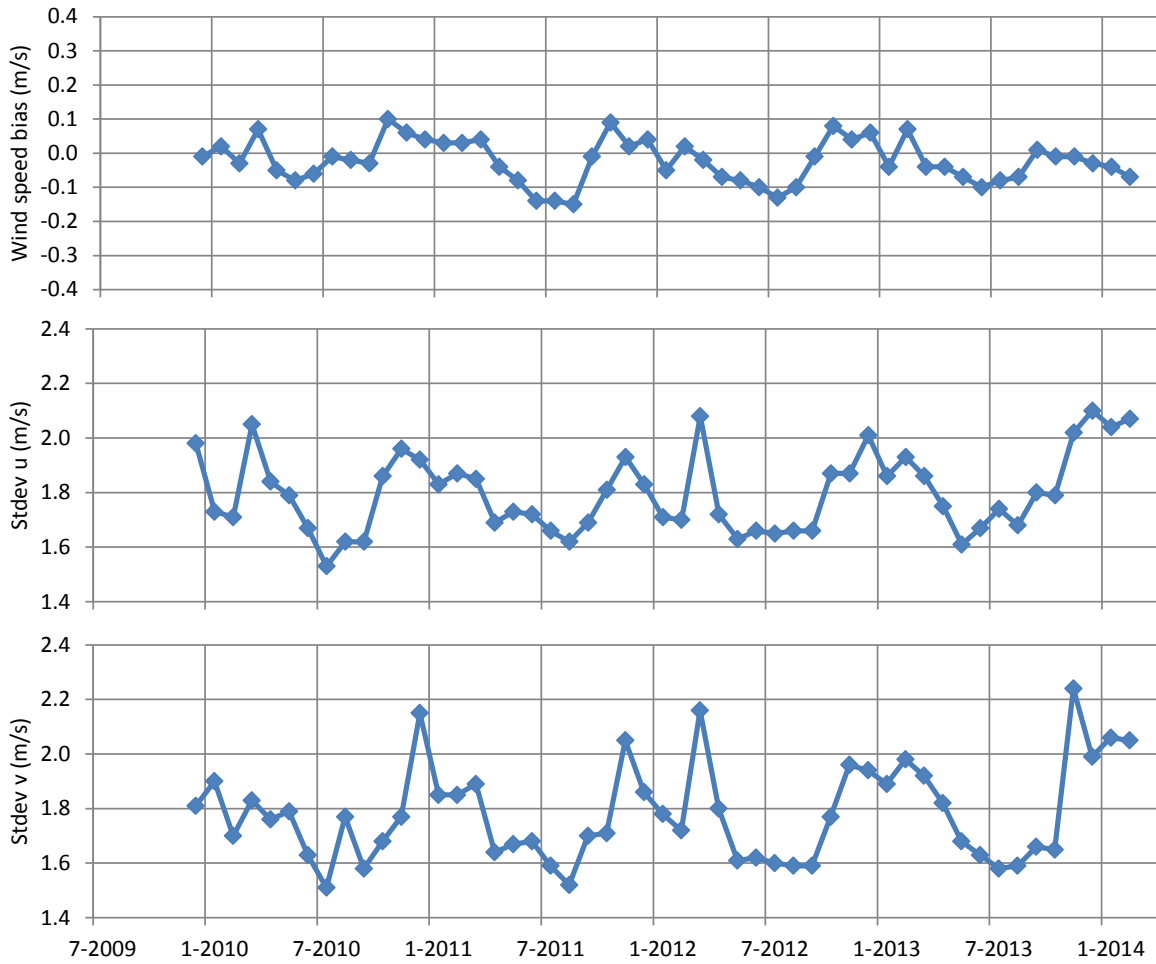


Figure 9: Wind speed bias (top), standard deviation of zonal wind component (middle) and standard deviation of meridional wind component (bottom) of 50 km OSCAT winds versus U10N buoy winds. The plotted values are monthly averages.

5 Triple collocation results

A triple collocation study was performed to assess the errors of the OSCAT, ECMWF and buoy winds independently. The triple collocation method was introduced by Stoffelen [16]. Given a set of triplets of collocated measurements and assuming linear calibration, it is possible to simultaneously calculate the errors in the measurements and the relative calibration coefficients. The triple collocation method can give the measurement errors from the coarse resolution NWP model perspective or from the intermediate resolution scatterometer perspective, but not from the fine resolution buoy perspective without further assumptions on the local buoy measurement error. A wind signal present in buoy measurements, but not in scatterometer measurements on the WVC scale, is therefore contained in the buoy error. This matter is extensively discussed by Vogelzang et al. [17].

Note that the ambiguity removal of OSCAT winds uses ECMWF wind forecasts as background. This might cause a very small influence on the selection of the OSCAT wind solution. However, in the 2DVAR ambiguity removal procedure the weight of the model winds is much lower than the weight of the observed winds. Therefore we are confident that the influence of model winds on scatterometer winds is very small, albeit strictly speaking not zero, and we can consider the scatterometer winds, buoy winds and model winds as independent.

Collocated data sets of OSCAT, ECMWF U10S and buoy U10N winds spanning the whole period of reprocessing were used in the triple collocation. Table 1 lists the error variances of the buoy, scatterometer and ECMWF winds from the intermediate resolution scatterometer perspective. For comparison, the results from the SeaWinds reprocessing [9] are also shown.

When we compare the 50 km OSCAT product with the 25 km OSCAT product, we see an increase of the buoy wind error standard deviations and a decrease of the ECMWF wind standard deviations. This is due to the coarser resolution of the 50 km product, which contains less small scale information and in this respect resembles better the ECMWF winds and resembles worse the buoy winds. The errors of the 25 km OSCAT winds are larger than those of the 50 km winds. This is most probably due to the larger noise in the 25 km wind retrievals. It is clear from Table 1 that the SeaWinds errors at 25 km and 50 km are significantly lower than those of OSCAT. Again, we attribute this to the lower instrument noise of SeaWinds. However, we note that the buoy error at the 25-km scale is smaller than the buoy error at the 50-km scale, which indicates that 25-km OSCAT resolves some buoy-measured variance not resolved by 50-km OSCAT.

In general, the OSCAT scatterometer winds are of good quality: at 25 km scale the error in the wind components is less than 0.8 m/s and at 50 km scale the errors are less than 0.6 m/s as is shown in Table 1.

	Scatterometer		Buoys		ECMWF	
	ϵ_u (m/s)	ϵ_v (m/s)	ϵ_u (m/s)	ϵ_v (m/s)	ϵ_u (m/s)	ϵ_v (m/s)
25 km OSCAT	0.80	0.71	1.44	1.45	1.33	1.40
50 km OSCAT	0.61	0.48	1.53	1.54	1.20	1.29
25 km SeaWinds	0.64	0.54	1.39	1.41	1.28	1.35
50 km SeaWinds	0.46	0.40	1.50	1.49	1.20	1.28

Table 1: Error standard deviations in u and v wind components from triple collocation of OSCAT and SeaWinds [9] 25 km and 50 km wind products with buoy and ECMWF forecast winds, seen from the scatterometer perspective.

From the triple collocation analysis, we can also determine the calibration of the scatterometer winds. The calibration coefficients a and b relate the observed scatterometer wind w to the ‘true’ wind t according to $t = a \times w + b$. This is done separately for the u and v wind components. The calibrations have been computed per year to see if there is any trend or glitch visible indicating instrument changes over time, see Figure 10. The years 2009 and 2014 have been neglected here since only few data are available in those years. The calibration coefficients indicate whether the scatterometer and ECMWF winds are underestimated ($a > 1$) or overestimated ($a < 1$). We see values close to 1, the slightly lower values for OSCAT indicate that the calibration or retrieval may be further adjusted. A small increasing trend appears to be present in the calibration coefficients (mainly of the meridional

winds) of both ECMWF and scatterometer wind components. This indicates that the ECMWF and scatterometer wind speeds gradually decrease when compared with the buoy winds, in line with the results from section 4.

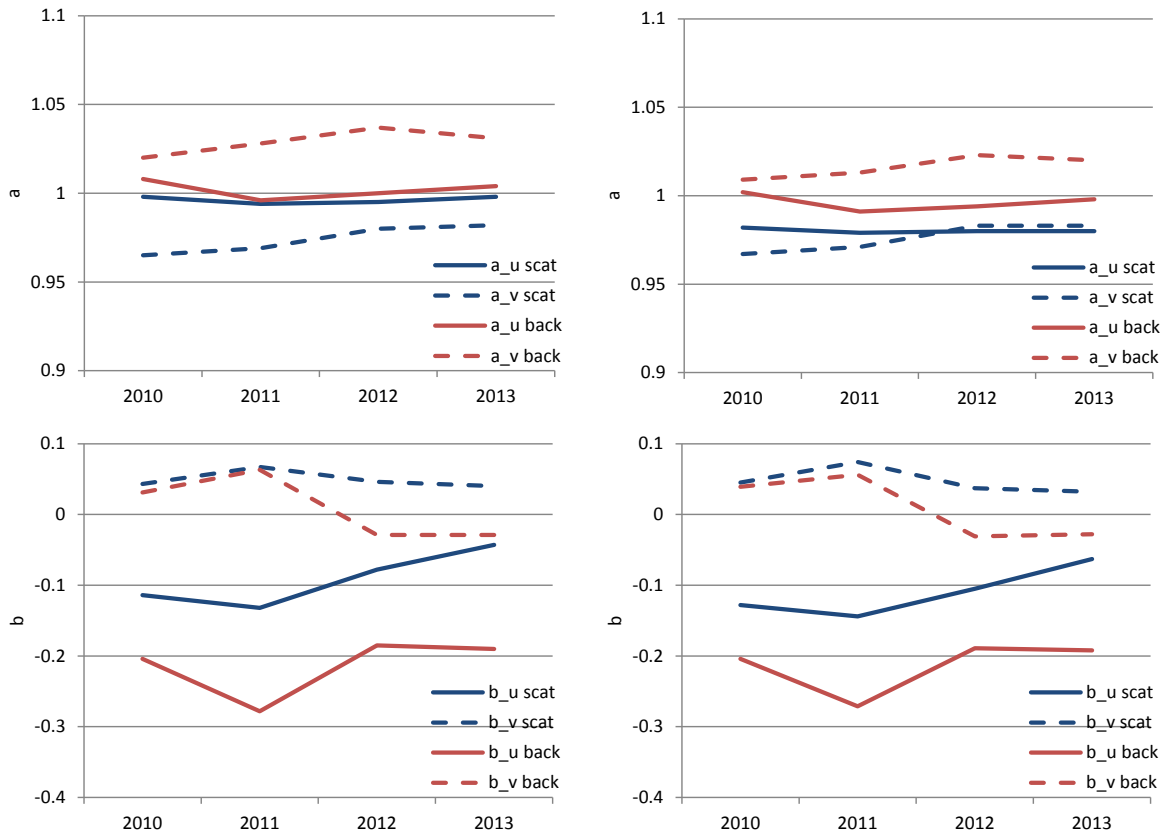


Figure 10: Triple collocation results for the wind component calibration coefficients *a* (top) and *b* (bottom) of the OSCAT 25 km (left) and 50 km (right) winds and the ECMWF winds relative to the buoy measurements, per year.

6 Conclusions

The quality and stability of the OSCAT CDR has been assessed by looking both at backscatter and wind data.

The backscatter values appear to be quite constant in time over a selected area on Antarctica, except for the first year of operations where we obtain higher values by approximately 0.2 to 0.4 dB. It is not clear whether this can be attributed to geophysical changes or to an instrument change. The observed change in backscatter could lead to an average wind speed decrease of approximately 0.3 m/s after 2010, but, although a decrease is indeed observed, it appears not fully compatible with the wind speed biases against ERA-Interim winds and buoy winds over time.

The scatterometer wind biases against moored buoy winds show a weak decrease of 0.05 to 0.10 m/s over the entire mission period of more than four years. The step which is observed in the backscatter data over Antarctic snow is not clearly visible in the wind speed biases at the buoy locations. ERA-interim winds appear rather stable in the OSCAT period.

The requirements as set by the World Climate Research Programme (WCRP) [18] are: accuracy better than 0.5 m/s, stability better than 0.1 m/s per decade. The accuracy requirement appears to be easily met by the OSCAT CDR, however the data record is too short to decide about the stability requirement. Still we think that this data record is a useful contribution to the collection of OSI SAF reprocessed wind data records. From the figures in section 4, we conclude that the OSI SAF product requirements ([1], better than 2 m/s in wind component standard deviation with a bias of less than 0.5 m/s in wind speed on a monthly basis) are also well met.

The triple collocation results show that the scatterometer winds are of good quality, reasonably well calibrated and sufficiently stable over the mission period.

7 References

- [1] OSI SAF,
Product Requirements Document
SAF/OSI/CDOP2/M-F/MGT/PL/2-001, 2016
- [2] OSI SAF,
Service Specification Document
SAF/OSI/CDOP2/M-F/MGT/PL/2-003, 2016
- [3] Padia, K.,
Oceansat 2 Scatterometer algorithms for sigma-0, processing and products format, version 1.1,
ISRO, April 2010
- [4] Vogelzang, J., A. Verhoef, J. Verspeek, J. de Kloe and A. Stoffelen,
PenWP User Manual and Reference Guide
NWPSAF-KN-UD-009, 2017
- [5] OSI SAF,
Oceansat-2 L2 winds Data Record Product User Manual
SAF/OSI/CDOP3/KNMI/TEC/MA/297, 2017
- [6] Kumar, R., S.A. Bhowmick, K. N. Babu, R. Nigam, and A. Sarkar,
Relative Calibration Using Natural Terrestrial Targets: A Preparation Towards Oceansat-2 Scatterometer
IEEE Transactions on Geoscience and Remote Sensing, 49, 6, 2268-2273, 2011,
doi:10.1109/TGRS.2010.2094196
- [7] Long, D. and M. Drinkwater,
Azimuth variation in microwave scatterometer and radiometer data over Antarctica
IEEE Transactions on Geoscience and Remote Sensing, 38, 4, 1857-1870, 2000,
doi:10.1109/36.851769
- [8] Jaruwatanadilok, S., B. Stiles and A. Fore,
Cross-Calibration Between QuikSCAT and Oceansat-2
IEEE Transactions on Geoscience and Remote Sensing, 52, 10, 6197-6204, 2014,
doi:10.1109/TGRS.2013.2295539
- [9] Verhoef, A., J. Vogelzang and A. Stoffelen,
Long-Term Scatterometer Wind Climate Data Records
IEEE Journal of Selected Topics in Applied Earth O, 10, 5, 2186-2194, 2017,
doi:10.1109/JSTARS.2016.2615873
- [10] Dee, D. et al.,
The ERA-Interim reanalysis: configuration and performance of the data assimilation system
Quarterly Journal of the Royal Meteorological Society, 137: 553–597, 2011, doi:10.1002/qj.828
- [11] Hersbach, H.,
Assimilation of scatterometer data as equivalent-neutral wind
ECMWF Technical Memorandum 629, 2010
- [12] Belmonte Rivas, M., A. Stoffelen, J. Verspeek, A. Verhoef, X. Neyt and C. Anderson,
Cone metrics: a new tool for the inter-calibration of scatterometer records
Accepted in IEEE Journal of Selected Topics in Applied Earth O, 2016
- [13] Bidlot J., D. Holmes, P. Wittmann, R. Lalbeharry, and H. Chen
Intercomparison of the performance of operational ocean wave forecasting systems with buoy data
Wea. Forecasting, vol. 17, 287-310, 2002
- [14] Liu, W.T., K.B. Katsaros, and J.A. Businger
Bulk parameterization of air-sea exchanges of heat and water vapor including the molecular constraints in the interface
J. Atmos. Sci., vol. 36, 1979
- [15] OSI SAF,
Algorithm Theoretical Basis Document for the OSI SAF wind products, version 1.4
SAF/OSI/CDOP2/KNMI/SCI/MA/197, 2017

- [16] Stoffelen, A.
Toward the true near-surface wind speed: error modeling and calibration using triple collocation
J. Geophys. Res. 103, C4, 7755-7766, 1998, doi:10.1029/97JC03180
- [17] Vogelzang, J., A. Stoffelen, A. Verhoef and J. Figa-Saldana
On the quality of high-resolution scatterometer winds
J. Geophys. Res., 116, C10033, 2011, doi:10.1029/2010JC006640
- [18] Global Climate Observing System,
Systematic Observation Requirements for Satellite-based Products for Climate Supplemental
details to the satellite-based component of the Implementation Plan for the Global Observing
System for Climate in Support of the UNFCCC - 2011 Update, December 2011, GCOS Report
154, <http://www.wmo.int/pages/prog/gcos/Publications/gcos-154.pdf>

8 Abbreviations and acronyms

2DVAR	Two-dimensional Variational Ambiguity Removal
ASCAT	Advanced Scatterometer
CDR	Climate Data Record
ECMWF	European Centre for Medium-Range Weather Forecasts
ERA	ECMWF re-analysis
EUMETSAT	European Organisation for the Exploitation of Meteorological Satellites
GTS	Global Telecommunication System
HH	Horizontal polarisation of sending and receiving radar antennas
ISRO	Indian Space Research Organisation
JPL	Jet Propulsion Laboratory
KNMI	Royal Netherlands Meteorological Institute
LKB	Liu, Katsaros and Businger
NWP	Numerical Weather Prediction
OSCAT	Scatterometer on-board the Oceansat-2 and ScatSat-1 satellites (India)
OSI	Ocean and Sea Ice
PenWP	Pencil beam Wind Processor
QC	Quality Control
QuikSCAT	US Quick Scatterometer mission carrying the SeaWinds scatterometer
SAF	Satellite Application Facility
SeaWinds	Scatterometer on-board QuikSCAT platform (USA)
u	West-to-east (zonal) wind component
v	South-to-north (meridional) wind component
U10N	Equivalent neutral wind at 10 meter height
U10S	Stress equivalent wind at 10 meter height
VV	Vertical polarisation of sending and receiving radar antennas
WCRP	World Climate Research Programme
WVC	Wind Vector Cell

9 Appendix A: List of used buoys

These are the buoy identifiers of the 106 buoys used in the validations and triple collocations in sections 4 and 5. The buoy locations can be looked up on <http://www.ndbc.noaa.gov/> and are shown in Figure 11. Only buoys yielding data in all of the four years from 2010 to 2013 have been used.

13002	32322	42019	44139	46083	51311	61002
13009	32323	42020	44141	46084	52001	62001
13010	41009	42035	44251	46086	52004	62029
15001	41010	42036	44255	46089	52073	62091
15002	41012	42039	46001	46132	52078	62092
15006	41013	42040	46004	46184	52079	62093
23001	41026	42057	46012	46205	52080	62094
23004	41036	42059	46015	46206	52082	62105
23007	41040	43001	46029	46207	52083	62163
31002	41041	43301	46036	46208	52084	64045
31004	41043	44009	46042	51003	52085	
31005	41046	44024	46050	51009	52086	
32303	41047	44025	46069	51015	52087	
32315	41048	44027	46075	51021	52088	
32316	42001	44037	46076	51303	52313	
32319	42003	44137	46082	51307	61001	

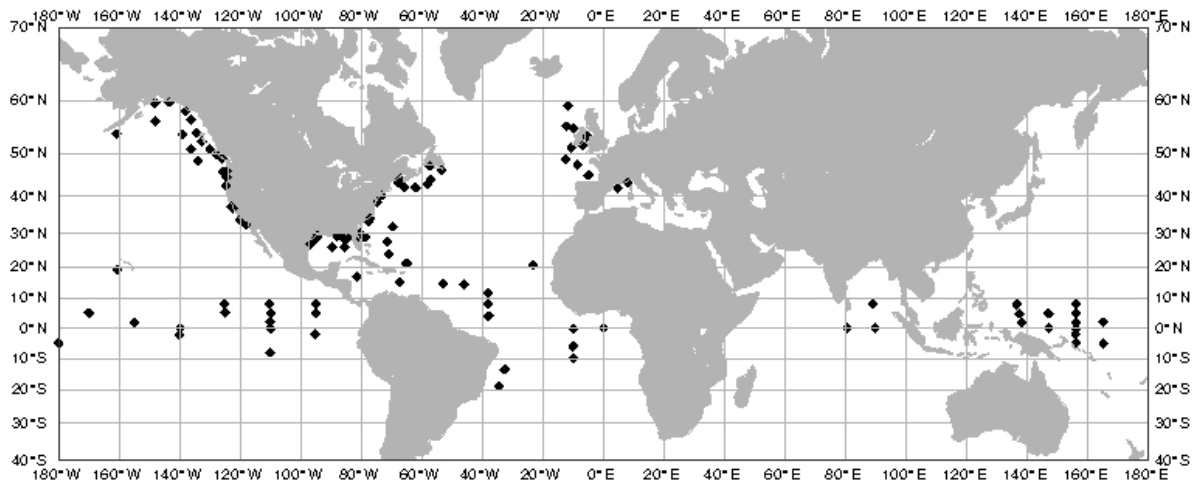


Figure 11: Location of the used buoys.